Online ISSN: 2981-0396 Print ISSN: 2981-0388

International Journal of Iron & Steel Society of Iran

Journal Homepage: https://journal.issiran.com/

Research Article

Investigation of the Properties and Microstructure of Direct Bonded Dolomite Refractory with Fe_2O_3-Cr_2O_3 Nanoparticles: A Comparative Study

A. Davoodi Jamaloei [*1], S. Ghasemi-Kahrizsangi [2], M. Barati [3]

Azar Refractory Products Company, Isfahan, Iran

ARTICLE INFO

Keywords:

Dolomite, Refractory, Fe_2O_3, Cr_2O_3, Nanoparticles.

Article history:

Received 10 June 2023
Received in revised form 16 June 2024
Accepted 09 March 2024

ABSTRACT

In this research, the properties and microstructure of direct bonded dolomite refractory (having) Iron oxide (Fe_2O_3) and Chrome oxide (Cr_2O_3) nanoparticles have been investigated. For this reason, 0, 0.5, 1, 1.5, 2, 2.5 and 3 wt. % of Fe_2O_3 and Cr_2O_3 nanoparticles have been added to the composition. After forming the samples as cylinders (50*50 mm^2), they were fired in an electric furnace at 1650 °C for 3 hr. The measured parameters were bulk density, apparent porosity, hydration resistance and cold crushing strength. Also, microstructural investigation and phase's analysis of the selected samples was performed by scanning electron microscopy (SEM/EDX) and X-ray diffraction (XRD) devices; respectively. Results showed that the use of Cr_2O_3 nanoparticles lead to formation of $CaCr_2O_4$ and $MgCr_2O_4$ phases, which improved the sintering process of the samples thorough the solid state sintering mechanism. Also, the use of Fe_2O_3 nanoparticles leads to creating $CaO.Fe_2O_3$ (CF) and $2CaO.Fe_2O_3$ (C_2F) phases which improved the sintering process of the specimen thorough the liquid phase sintering mechanism. Also, it showed that Cr_2O_3 nanoparticles additive has a greater effect on improving the properties of direct bonded dolomite specimens compared to Fe_2O_3 nanoparticles additive.

1. Introduction

Existence of abundant resources of dolomite in the world, high refractoriness, ability to produce clean melt by removing sulfur and phosphorus impurities of molten, etc. are the advantages of using dolomite refractories in various industries [1-6]. But in addition to the more advantages of dolomite products, the low hydration resistance of them has created a great challenge for using these types of refractories [1-4, 7,8]. Thus, some efforts have been done to decrease this weakness of dolomite-based products. Among the proposed solutions is the use of organic materials such as pitch and bitumen to cover the surface of dolomite grains and lead to the covering surface of dolomite bricks from reaching moisture to them [1-6, 9-11]. The other way is carbonation of the external surfaces of dolomite bricks with the help of carbonate based-compounds. The most important solution that has been considered by researchers in recent years is the use of oxides of various compounds such as ZrO_2, TiO_2, $MgAl_2O_4$, CuO, $FeTiO_3$, SiO_2, Al_2O_3, V_2O_5, CeO_2 and La_2O_3 [1-24]. The results of experiments have shown that the latest way has better impact than the other mentioned ways. Researchers have noted that the use of oxide compounds such as zirconium and titanium has led to the formation of high

*Corresponding author
Email: davoodi.a.j@gmail.com
Address: Azar Refractory Products Company, Isfahan, Iran
1. Ph.D, 2. MSc, 3. MSc

DOI: http://10.22034/IJISSI.2024.2004464.1266
Published by ISSI (Iron & Steel Society of Iran)

melting point phases which improved sintering process through the solid-state mechanism sintering [2, 3, 9, 14, 24]. While the use of some other oxides such as silica and aluminum cause the formation of low melting point phases and improve the sintering process through the liquid state mechanism sintering [2, 8, 10]. The purpose of this paper is the investigation the effect of using iron and chrome oxide nanoparticles on the microstructure and properties of the direct bond dolomite samples. Also the sintering mechanism of each of them has also been evaluated.

2. Method of experiment

2.1. Raw materials

a) Sintered dolomite (CaO.MgO): sintered dolomite, extracted from the Shadiyar mine in Iran, used as the main component in this research. Table 1. shown the chemical analysis of it.
b) Binder: liquid paraffin (3 wt. %) with the technical specifications mentioned in Table 2. was used as a binder in this research.
c) Nano-iron oxide (Fe_2O_3) and nano-chrome oxide (Cr_2O_3): Iron and chrome oxide nanoparticles were used as additives in this study. The transmission electron microscopy (TEM) image and chemical analysis of them presented in Fig. 1. and Table 3. respectively.

2.2. Forming, drying and firing process of the samples

The prepared samples with the mentioned formulation in Table 4. were pressed in a cylindrical shape with the dimension of 50 * 50mm^2. They were dried (at110 °C for 24hr) and then sintered (at 1650°C for 3 hr).

2.3. Tests

a) Physical properties:
The physical properties test such as bulk density (BD), apparent porosity (AP) and resistance to hydration (HR) were performed according to the ASTM C20-87 and ASTM C492 standards; respectively.
b) Mechanical properties:
The cold compressive strength (CCS) test was performed according to the ASTMC133-84 standard.

2.4. Phases and microstructural analysis

The phases and microstructural evaluation were performed on the selected samples using XRD and SEM/EDX devices; respectively.

Table 1. Chemical analysis of sintered dolomite.

Oxide	CaO	MgO	SiO_2	Fe_2O_3	Al_2O_3	LOI
(wt. %)	57.68	39.8	0.94	1.08	0.26	---

Table 2. Technical specifications of liquid paraffin.

Properties	Value
Viscosity(CPS)at 25°C	8500-9000
Specific Gravity at 25°C	1.25
Fixed Carbon (%)	48.2
Non-Volatile Matter (%)	81.12
Moisture	<0.5

Table 3. Properties of nano-iron oxide (Fe_2O_3) and nano-chrome oxide (Cr_2O_3) particles.

Oxide	Purity (%)	Size (nm)	Density (g/cm^3)	SSA (m^2/g)	Color	CAS number	supplier
Fe_2O_3	>98	40-50	5.24	115	red	1309-37-1	Us research nanomaterial's, INC.
Cr_2O_3	>99	50-60	5.22	>80	green	1308-38-9	Us research nanomaterial's, INC.

Table 4. Formulation of prepared specimens.

additives	reference	Nano-Fe_2O_3	Nano-Fe_2O_3	Nano-Fe_2O_3	Nano-Fe_2O_3	Nano-Fe_2O_3	Nano-Fe_2O_3	Nano-Cr_2O_3	Nano-Cr_2O_3	Nano-Cr_2O_3	Nano-Cr_2O_3	Nano-Cr_2O_3	Nano-Cr_2O_3
wt.%	0	0.5	1	1.5	2	2.5	3	0.5	1	1.5	2	2.5	3
Sample Code	D	$DF_{0.5}$	DF_1	$DF_{1.5}$	DF_2	$DF_{2.5}$	DF_3	$DCr_{0.5}$	DCr_1	$DCr_{1.5}$	DCr_2	$DCr_{2.5}$	DCr_3

3. Results and discussion

3.1 Phase's analysis

3.1.1. Sample without additive (D)

TEM images of the Fe_2O_3 and Cr_2O_3 nano materials are shown in Fig. 1. X-ray Diffraction patterns (XRD) of the sample without additive (D) shows that only two main phases, i.e. Calcia (CaO) and magnesia (MgO) is detected (Fig. 2.). Also, detection of some weak picks, related to $Ca(OH)_2$ phase, demonstrated the high tendency of this sample to absorb humid and hydration.

3.1.2. Samples with iron oxide ($DF_{1.5}$ and DF_3)

X-ray diffraction patterns (XRD) related to samples containing 1.5 and 3 wt. % nano-iron oxide after firing are shown in Figs. 3.(a-b). In addition to Calcia (CaO) and Magnesia (MgO) phases, some picks related to phases with low melting point like $CaO.Fe_2O_3$ (CF) and $2CaO.Fe_2O_3$ (C_2F) are detected by increasing the amount of nano-iron oxide. Simultaneously with decreasing the intensity of Calcia (CaO) and magnesia (MgO), peaks intensity of $CaO.Fe_2O_3$ (CF) and $2CaO.Fe_2O_3$, (C_2F) phases are decreased for higher content nano-iron oxide at firing temperature. Generation of $CaO.Fe_2O_3$ (CF) and $2CaO.Fe_2O_3$ (C_2F) phases with low melting point at the firing temperature (1650°C) leads to the improvement of the sintering process by liquid phase mechanism and thus leads to the decrement of the voids, porosities and finally hydration resistance will be enhanced. Also, not detection picks of $Ca(OH)_2$ phases in X-ray diffraction patterns show the impact of iron

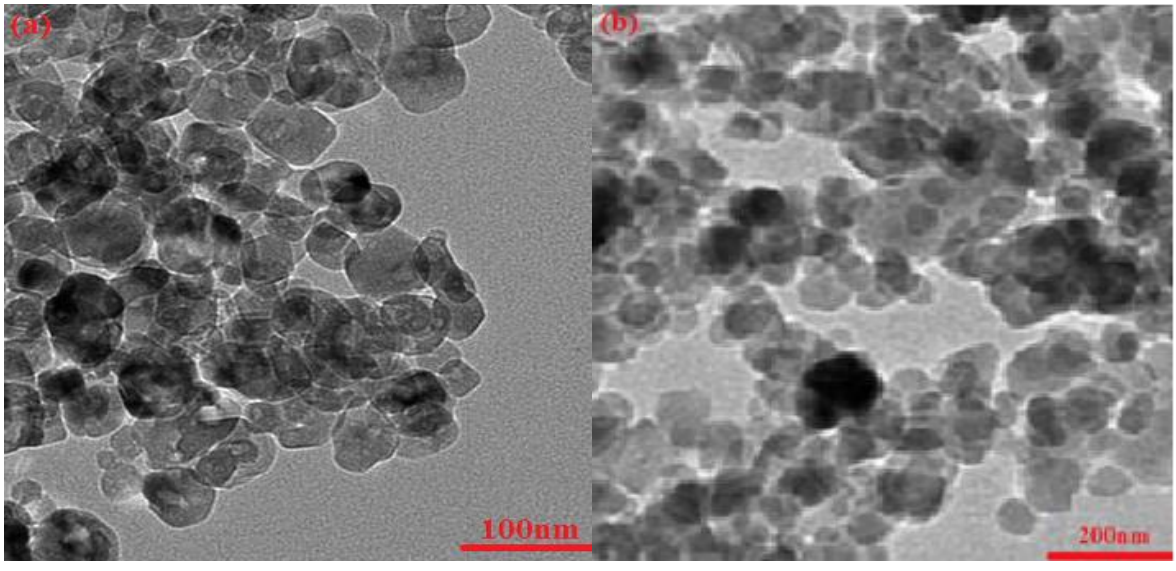

Fig. 1. TEM images of the a) nano-Fe_2O_3, and b) nano-Cr_2O_3.

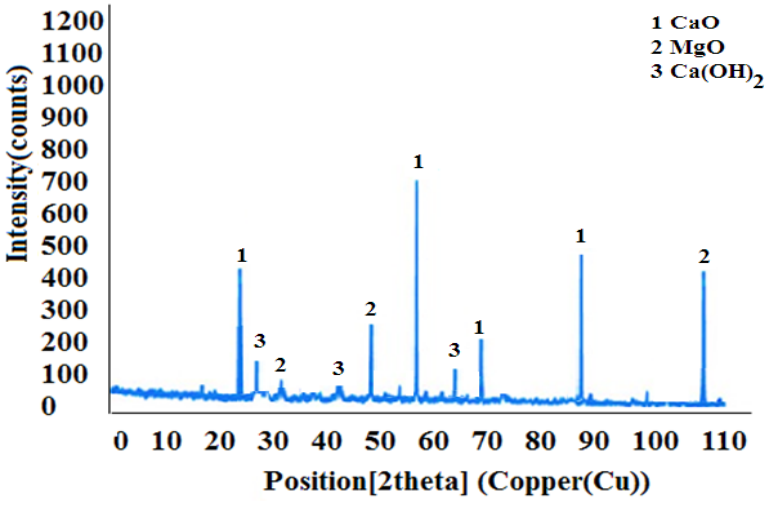

Fig. 2. X-ray diffraction patterns (XRD) related to D sample.

oxide addition on hydration resistance improvement of samples.

3.1.3. Samples with chrome oxide ($DCr_{1.5}$ and DCr_3)

The X-ray diffraction patterns (XRD) related to samples containing 1.5 and 3 wt. % nano-chrome oxide after firing process are shown in Figs. 4.(a-b). Calcia (CaO) and magnesia (MgO), $CaCr_2O_4$ and $MgCr_2O_4$ phases detected as the main crystalline phases in these samples. The melting point of $MgCr_2O_4$ and $CaCr_2O_4$ phases are 2350 °C and 2170 °C; respectively [4]. In during the firing process (1650 °C), the $CaCr_2O_4$ and $MgCr_2O_4$ phases are in solid state. Generated $MgCr_2O_4$ and $CaCr_2O_4$ phases preferred to locate on intra-granular and inter-granular area of magnesia (MgO) and Calcia (CaO) grains. The peaks intensity of the $MgCr_2O_4$ and $CaCr_2O_4$phaseS for DCr_3 sample are higher than other samples contain chrome oxide.

3.2. Scanning electron microscopy results

3.2.1. Sample without additive (D)

By comparing the scanning electron microscopy (Fig. 5a.), it can be seen that the grain boundary and porosities of this sample (D point) is more in compare to other samples.

3.2.2. Samples with Iron oxide ($DF_{1.5}$, DF_2 and DF_3)

It is observable that containing nano-iron oxide samples ($DF_{1.5}$ and DF_3), have fewer voids and porosity

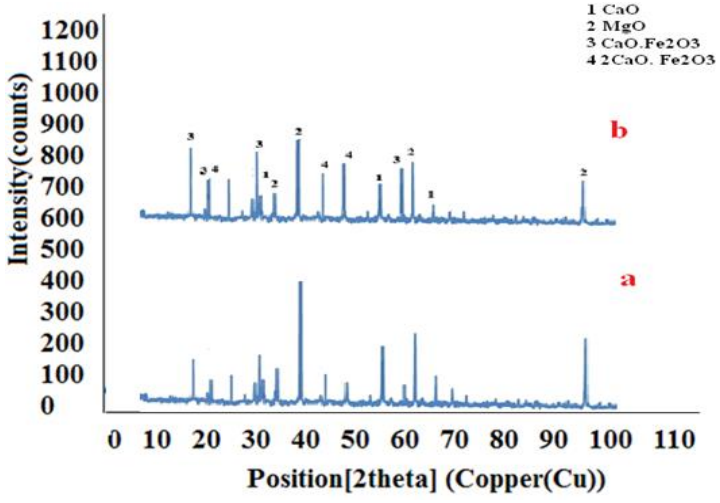

Fig. 3. X-ray diffraction patterns (XRD) related to a) $DF_{1.5}$ and b) DF_3 samples.

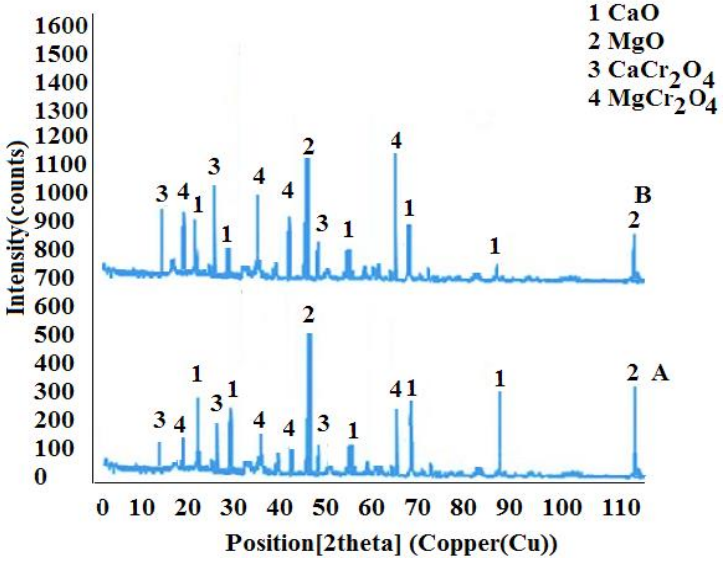

Fig. 4. X-ray diffraction patterns (XRD) related to a) $DCr_{1.5}$ and b) DCr_3 samples.

than (D) sample (Figs. 5.(b-c)). By using of EDX analysis results (Table 5.), it can be concluded that A points (dark gray) is related to magnesia (MgO) phase (for to low atomic number), B points (light gray) is related to Calcia (CaO) phase (for to high atomic number), and C points (white regions at the grain-boundaries) are related to phases which have low melting point, such as CaO. Fe_2O_3 (CF) and $2CaO.Fe_2O_3$ (C_2F) phases. Also, it is observable (Figs. 5.(a-c)) that magnesia (MgO) and Calcia (CaO) grains grow by adding nano-Iron oxide. Grain-grown of magnesia (MgO) and Calcia (CaO) grains leads to grain-boundaries, porosities, and triple intersection points to be reduced. Thus, the hydration resistance is enhanced. Based on the above mentioned, specification of liquid phase sintering mechanism such as continuity and high quantity of the melted phase, also separated small porosities are observable for samples with the highest content of Iron oxide.

3.2.3. Samples with Chrome oxide ($DCr_{1.5}$, $DCr_2$and DCr_3)

For samples with higher than nano-chrome oxide content (DCr_3), a homogeneous microstructure

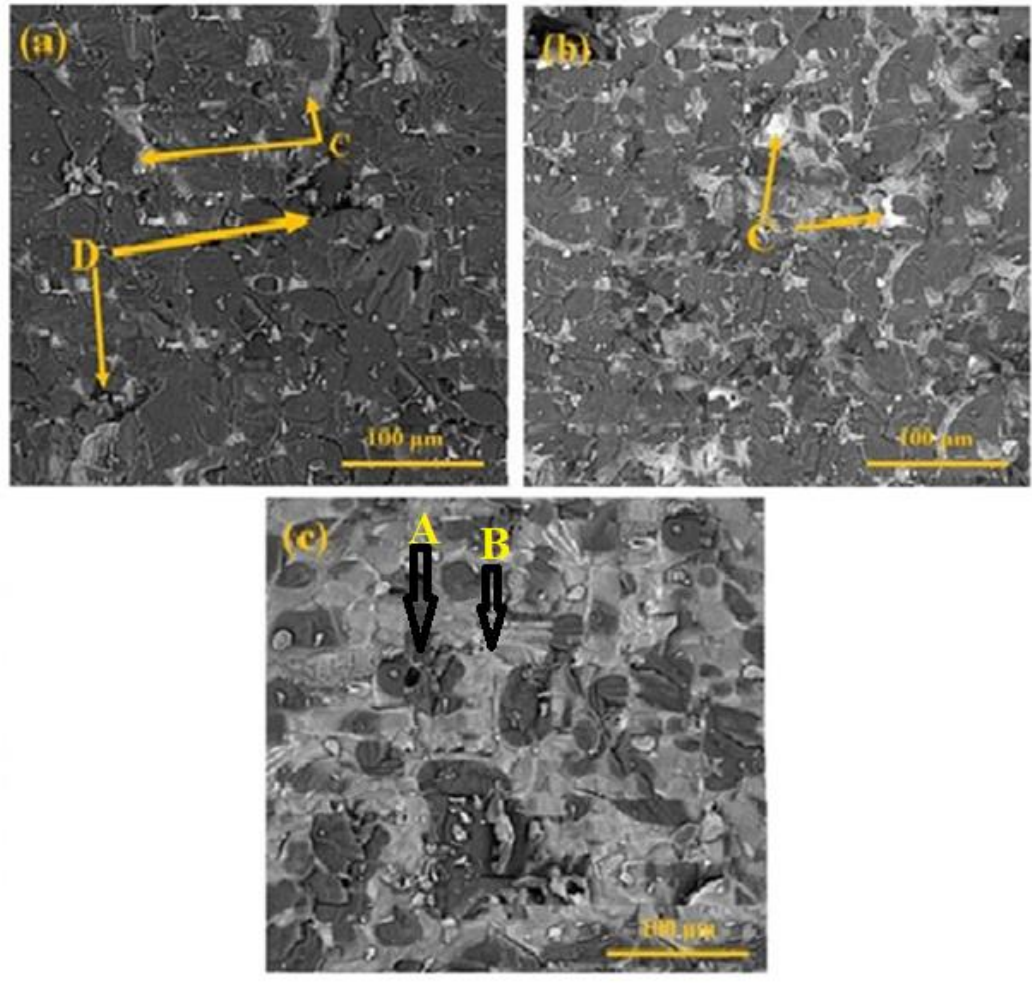

Fig. 5. SEM images of fractured surfaces of the samples: (a) D, (b) $DF_{1.5}$ and (c) DF_3.

Table 5. EDX analysis of A, B and C points related to Fig. 5.

Element	Point A (wt %)	Point B (wt %)	Point C (wt %)
O	38.20	22.42	69.35
Mg	61.65	-	1.56
Si	-	-	2.96
Ca	-	57.39	15.15
Fe	-	19.8	1.7
Al	-	-	9.1
Au	0.24	0.59	0.18

composed mainly of a well-distributed phases is observed (Figs. 6.(a-b)). It's observable that two phases are surrounded by the magnesia (MgO) and Calcia (CaO) ground mass. The first one is related to light gray particles composed by Ca and Cr elements, as it was identified by EDS. This phase is a $CaCr_2O_4$ spinel which detected with XRD analysis . The last phase is related to bright gray particles composed by Mg and Cr elements (identified by the EDS), (Table 6.). This phase is $MgCr_2O_4$ spinel which detected with XRD analysis. By increasing nano-chrome oxide content, some coarse agglomerations composed by $CaCr_2O_4$ and $MgCr_2O_4$ were created.

4. Physical properties

4.1 Densification

4.1.1. Samples without and containing nano-iron oxide

Variation of bulk density and apparent porosity of without and containing nano-iron oxide samples are shown in Fig. 7. It is observable that bulk density and apparent porosity increased and decreased; respectively. This variation trend is related to filling up pores, porosities and inter-grain pores of samples matrix by Iron oxide with formation of low-melting point phases such as CaO. Fe_2O_3 (CF) and $2CaO.Fe_2O_3$ (C_2F) phases.

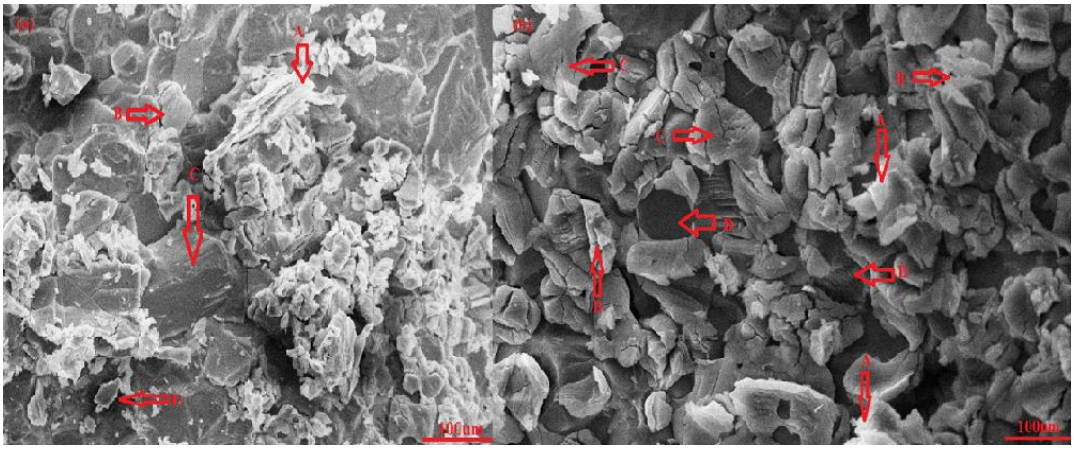

Fig. 6. SEM images of fractured surfaces of the samples: (a) $DCr_{1.5}$ and (B) DCr_3.

Table 6. EDX analysis of A, B, C and D points related to Fig. 6.

Element	Point A (wt %)	Point B (wt %)	Point C (wt %)	Point D (wt %)
O	37.19	38.54	43.73	45.65
Mg	62.64	-	0.52	15.30
Si	-	-	0.41	0.11
Ca	-	61.36	18.15	0.8
Cr	-	---	34.46	32.60
Al	-	-	2.60	5.42
Au	0.17	0.19	0.13	012

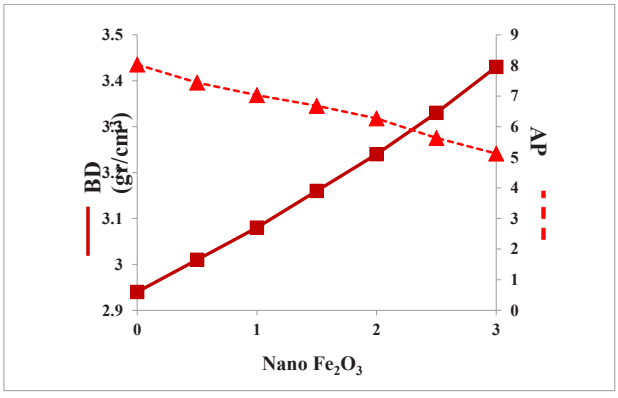

Fig. 7. Variation of bulk density and apparent porosity of without and containing nano-iron oxide samples.

4.1.2. Samples with chrome oxide

Bulk density and apparent porosity variation of the fired samples with different amount of nano-chrome oxide have been shown in Fig. 8. It is showed that the bulk density starting to increase gradually from 0 up to3 wt. %. This increment can be attributed to:

- Filling up of the inter-granular voids between Calcia (CaO) and magnesia (MgO) grains and creating a better compression of the microstructure of samples.
- A better firing of the refractory matrix due to the presence of chrome oxide.
- The higher true density of nano-chrome oxide (5.22 g/cm^3) , in comparison to the Calcia (3.35 g/cm^3) and magnesia (3.58 g/cm$_3$) or maybe due to a possible new phases formation [such as $CaCr_2O_4$ (4.43 g/cm^3) and $MgCr_2O_4$ (4.43 g/cm^3)] [4].
- And nano-chrome oxide alter the grain boundary between assemblage and the morphology of the grains, changing the dihedral angle (θ). The lowering of the dihedral angle means Υ_{ss} will be smaller, which will facilitate grain-to-grain contact and ultimately direct bond formation. This tendency increases the densification.

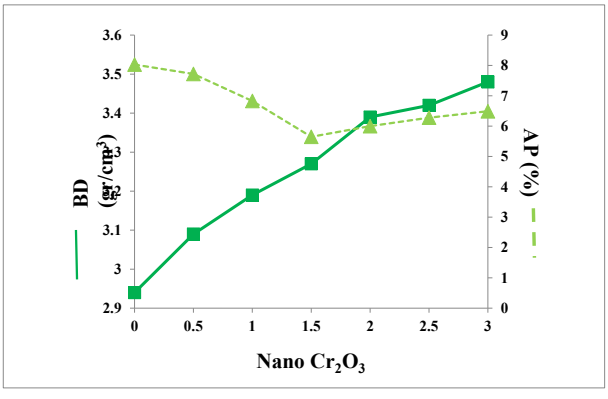

Fig. 8. Variation of bulk density and apparent porosity of without and containing nano-chrome oxide samples.

But the apparent porosity variation shows that it values decrease with increasing nano-chrome oxide content up to 1.5 wt.% and for further nano-Cr_2O_3 (2 up to 3 wt.%), the apparent porosity increased. The reason for this variation is more differences in thermal expansion coefficients between magnesia (~13.5 × 10^{-6} °C^{-1}), (CaO) (~13.8~ × 10^{-6} °C^{-1}) and $MgCr_2O_4$ (~8.5~ × 10^{-6} °C^{-1}) phases, which cause to generation high amount of micro-cracks in the microstructure.

5. Hydration resistance

5.1. Samples without and containing nano-iron oxide

The hydration resistance variation of the samples are shown in Fig. 9. It is showed that the variation of weigh gained of sample decreased with increasing the amount of nano-iron oxide appreciably.

Generally the reasons for hydration resistance enhancement of sample containing nano-iron oxide are due to:

- The promotion of densification by the addition of nano-iron oxide due to decrement the active specific area of main grains (Calcia and magnesia)
- By adding of nano-iron oxide, the content of free Calcia phase (CaO) in samples decreased further.
- It has been proven that the hydration reaction always starting from the area with crystal defect. Thus, the grain-boundaries and triple points are the poor hydration resistance area. Therefore, by adding nano-Iron oxide, some phases such as $CaO.Fe_2O_3$ (CF) and $2CaO.Fe_2O_3$ (C_2F) with low melting point formed and located at these are, thus preventing the hydration of the samples.

5.2. Samples with chrome oxide

Fig. 9. shows that the weight gained of samples decreased appreciably with addition of nano-chrome oxide. When nano-chrome oxide was added, the hydration resistance of the samples is increased. This improvement is due to generation of phases such as $MgCr_2O_4$ and $CaCr_2O_4$ which located at triple point and grain-boundaries of CaO and MgO grains, thus preventing the hydration resistance of samples and the other reason is converted of CaO and MgO free phases to high hydration resistance phases i.e. $MgCr_2O_4$ and $CaCr_2O_4$.

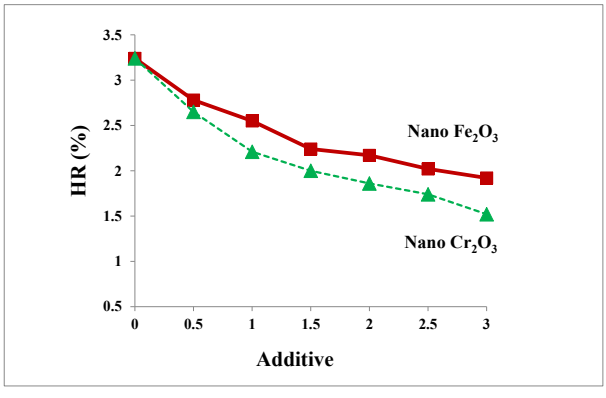

Fig. 9. The hydration resistance variation of without and containing nano-iron and nano-chrome oxide samples.

6. Mechanical properties

6.1. Cold Crushing Strength (CCS)

6.1.1. Samples without and containing nano-Iron oxide

Typically, cold crushing strength (CCS) test results of samples are used for assessment of firing process.

Usually, a higher amount of strength indicates a more complete and better firing process. Fig. 10. shows that D and DF3 samples have the lowest and highest CCS values; respectively. The lowest CCS value is due to the heights porosities, pores, and grain-bindery and low-bond connections between main grains. Also, the use of nano-iron oxide lead to improve the firing process by liquid phase sintering mechanism and created a strong bonds connection between CaO and MgO grains through the generation of some phases with low melting point such as $CaO.Fe_2O_3$ (CF) and $2CaO.Fe_2O_3$ (C_2F).

6.1.2. Samples with nano-chrome oxide

The results of cold crushing strength of the samplers containing nano-chrome oxide are shown in Fig. 10. The cold crushing strength value is increased with adding nano-chrome oxide content up to 1.5 wt. %. The highest CCS value was registered for the $DCr_{1.5}$ sample (843 kg/cm^2). Good compactness created by the nano-chrome oxide particles and the low values of apparent porosity are the reasons for this upgraded. Also it was showed that for higher nano-chrome oxide concentrations (from 2 to 3 wt. %), the CCS values were decreased. The reason for these drops may be attributed to the:

- Formation of coarse agglomerates and a large thermal expansion coefficient miss-match between different existing phases which leads to generation of micro-cracks around agglomerates; these micro-cracks could be a detriment to CCS, as can be observed in the plot of Fig. 10.

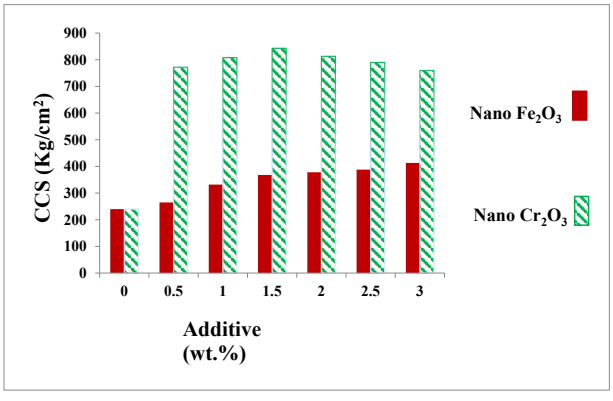

Fig. 10. The variation of CCS of without and containing nano-iron and nano-chrome oxide samples.

7. Conclusions

In this paper, the properties and microstructure of direct bonded dolomite refractory using nano-Fe_2O_3 and nano-Cr_2O_3 has been investigated. The following results are concluded:

- Adding nano-iron oxide to dolomite specimens leads to the generation of some phases with low melting point, such as $CaO.Fe_2O_3$ (CF) and $2CaO.Fe_2O_3$ (C_2F). These phases improved the sintering process through the liquid state mechanism of sintering.
- The use of nano-iron oxide leads to the improvement hydration resistance of samples due to alternation of free-Calcia and magnesia, generation of low melting point phases and filling up voids and porosities in the microstructure.
- The use of nano-chrome oxide improved the sintering process of samples through the solid state sintering mechanism.
- Generation of $MgCr_2O_4$ and $CaCr_2O_4$ phases, improved the properties of samples containing nano-chrome oxide.
- Generally, nano-chrome oxide has higher than effect on properties improvement of samples than iron oxide.

References

[1] Kahrizsangi S.G.h, Nemati A, Shahraki A, Farooghi M, The effect of nano-additives on the hydration resistance of materials synthesized from the MgO-CaO system, Intentional Journal of Engineering , 2016; 29: 539-545.
[2] Ghasemi-Kahrizsangi S, Gheisari Dehsheikh H, Karamian E, Nemati A, A comparative evaluation of the addition impact of nanometer-sized tetravalent oxides on the performance of Doloma-Magnesia ceramic refractories, Ceramics International. 2018; 44(2): 2058-2064.
[3] Boroujerdnia M, Ghasemi-kahrizsangi S, Gheisari-dehsheikh H, The effect of nano meter size ZrO_2 particles addition on the densification and hydration resistance of magnesite– dolomite refractories, Iranian Journal of Materials Science and Engineering. 2016; 13(4): 33-40.
[4] Ghasemi-Kahrizsangi S, Gheisari Dehsheikh H, Boroujerdnia M, MgO–CaO–Cr_2O_3 composition as a novel refractory brick: Use of Cr_2O_3 nanoparticles, Boletín de la Sociedad Española de Cerámica y Vidrio. 2017; 56(2): 83-89.
[5] Ghasemi-Kahrizsangi S, Karamian E, Gheisari Dehsheikh H, The impact of $ZrSiO_4$ nanoparticles addition on the microstructure and properties of dolomite based refractories, Ceramics International. 2017; 43(16): 13932-13937.
[6] Ghasemi-Kahrizsangi S, Gheisari Dehsheikh H, Karamian E, Boroujerdnia M, Payandeh K.h, Effect of $MgAl_2O_4$ nanoparticles addition on the densification and properties of MgO-CaO refractories, Ceramics International. 2017; 43(6): 5014-5019.
[7] Ghasemi-Kahrizsangi S, Karamian E, Gheisari-Dehsheikh H, Ghasemi-Kahrizsangi A, A Review on Recent Advances on Magnesia-Doloma Refractories by Nano-Technology, Journal of Water and Environmental Nanotechnology. 2017; 2(3): 2020-206.
[8] Shahraki A, Ghasemi-Kahrizsangi S, Nemati A, Performance improvement of MgO-CaO refractories by the addition of Nano-sized Al_2O_3, Material Chemistry and Physic.2017; 198: 354-359.

[9] Ghasemi-Kahrizsangi S, Shahraki A, Farooghi M, Effect of nano-TiO_2 additions on the densification and properties of Magnesite–Dolomite ceramic composites, Iranian Journal of Society and Technology, Trans A. 2016: 1-9.
[10] Gheisari Dehsheikh H, Ghasemi-Kahrizsangi S, The influence of silica nanoparticles addition on the physical, mechanical, thermo-mechanical as well as microstructure of Mag-Dol refractory composites, Ceramics International. 2017; 43(18): 16780-16786.
[11] Gheisari Dehsheikh H, Ghasemi-Kahrizsangi S, Karamian E, Addition impact of nano-carbon black on the performance of MgO.CaO compounds, Ceramics International. 2018; 44(1): 5524-5527.
[12] GKahrizsangi S, Nemati A, Shahraki A, Farooghi M, Effect of nano-sized Fe_2O_3 on microstructure and hydration resistance of MgO-CaO refractories, International Journal of Nano science and Nanotech logy. 2016; 12 (1): 19-26.
[13] Ghasemi-Kahrizsangi S, Nemati A, Shahraki A, Farooghi M, Densification and properties of Fe_2O_3 nanoparticles added CaO refractories, Ceramics International. 2016; 42: 12270-12275.
[14] Ghasemi-Kahrizsangi S, Barati M, Gheisari H, Shahraki A, Farooghi M, Densification and properties of ZrO_2 nanoparticles added magnesia–doloma refractories, Ceramics International.2016; 42(14): 15658-15663.
[15] Ghasemi-Kahrizsangi S, Karamian E, Ghasemi-KahrizsangiA, Gheisari Desheikh H, Soheily A, The impact of trivalent oxide nanoparticles on the microstructure and performance of magnesite-dolomite refractory bricks, Material Chemistry and Physics. 2017; 193: 413-420.
[16] Gheisari Dehsheikh H, Karamian E, Owsalou R.G.h, Ghasemi-Kahrisangi S, Vefgh N, Soheily A, Improvement in performance of MgO–CaO refractory composites by addition of Iron (III) oxide nanoparticles, Ceramics International. 2018; 44(13): 15880-15886.
[17] Zhang H, Zhao H, Chen J, Li J, Yu J, Nie J, Defect study of MgO-CaO material doped with CeO, Hindawi Publishing Corporation Advances in Materials Science and Engineering. 2013: 673786-5.
[18] Ghosh A, Bhattacharya T.K, Mukherjee B, Tripathi H. S, Das S.K, Effect of Fe_2O_3 on the densification and properties of lime, Ceramics −Silikáty. 2003; 47 (2): 70-74.
[19] Hadian M, Nazari B, Influence of magnesia addition on hydration of iranian dolomite, Iranian Journal of Materials Science & Engineering. 2010; 7(30).
[20] lee J, Choi H.S, Lee S.j, effect of Fe_2O_3 addition on the hydration resistance of CaO, Journal of Ceramic Processing Research. 2012; 13(5): 6406-650.
[21] Ghosh A, Bhattacharaya T.k, Maiti S, Mukherjee B, Tripathi H.S, Das S.k, Densification and properties of lime with V_2O_5 addition, Ceramics International 30. 2004: 2117-2120.
[22] Ghosh A, Bhattacharaya T.k, Maiti S, Mukherjee B, Tripathi H.S, Das S.k, solid state sintering of lime in presence of La_2O_3 and CeO_2, Bulletin, Material, Society. 2003; 26: 703–706.
[23] Chen Sh, Lu P, improved hydration resistance of synthesized magnesia–calcia clinker by surface modification, Journal of American Ceramic Society. 2004; 87(12): 2164–2167.
[24] Chen M, Lu C, YU J, improvement in performance of MgO-CaO refractories by addition of nano –ZrO_2, Journal of the European Ceramic Society. 2007; 27: 4633-4638.